by the trace water in the medium.[5c] UV–vis and FTIR spectra at the end of the electrolysis period show that the catalyst remains unchanged during the electrolysis experiments.

The kinetics of CO_2 reduction were studied by computer simulation of the scan rate dependence of cyclic voltammetric wave shapes under conditions where the concentrations of *cis*-$[Os(bpy)_2(CO)H][PF_6]$, CO_2, and H_2O could be systematically varied.[6] Of a variety of possible mechanistic cases that were considered, the data were most satisfactorily fit by a mechanism that involves an initial, irreversible reaction between $[Os(bpy)_2(CO)H]^-$ and CO_2 with a rate constant, k_1, to give an intermediate which subsequently undergoes either a self-reaction or an irreversible reaction with H_2O as shown in eq 1–8 (Scheme I). In one alternate mechanism, which gives a similar variation in $i_d/i_{cat.}$ with concentration, see below, but with a less satisfactory fit, parallel pathways exist which are first order in *cis*-$[(bpy)_2Os(CO)H][PF_6]$ and CO_2 with one of the two pathways involving a following step which is first order in added H_2O. As shown, the mechanism does not include the H_2 production pathway which appears at high $[H_2O]$. In principle, it should have been possible to use product ratio studies at high added $[H_2O]$ to evaluate k_6 and k_7. However, there are large uncertainties in the analyses, and we have insufficient data to justify using the results in this way.

In Figure 1B is shown a plot of the ratio of the diffusion and catalytic currents measured at the second wave ($i_d/i_{cat.}$) vs the function log $(RT[CO_2]/F\nu)$ at various assumed values of k_1 where ν is the scan rate and F the Faraday constant. This concentration–scan rate function is appropriate for the mechanism in eq 1–4 in the absence of added H_2O. The variation of $i_d/i_{cat.}$ with added water is consistent with the additional steps proposed in the mechanism (see Figure 1C). The combination of results from the kinetic and product studies suggests that formate arises from the H_2O branch (reaction 5 followed by reaction 6) and CO from both branches.

When the isotopically labeled complex *cis*-$[Os(bpy)_2(CO)D][PF_6]$ was used as a catalyst under conditions where formate production is nearly maximized (0.3 M added H_2O), there was no proton incorporation after 1.8 turnovers of formate. Likewise, in experiments using $^{13}CO_2$ there was no incorporation of ^{13}CO into the catalyst after 5.5 turnovers in terms of the production of CO. The labeling studies are consistent with the mechanism in eq 1–8 and rule out pathways like insertion of CO_2 into the Os–H bond. They show that the –CO and –H groups in the proposed intermediates I_a and I_b are inert and are not involved in the net reductions.

In dry CH_3CN[5a] where the formate pathway is negligible, similar current enhancements at the second bpy wave are observed for the related complexes *cis*-$[M(bpy)_2(CO)R]^+$ (M = Os, R = Me or Ph; M = Ru, R = CH_2Ph) and *trans*-$[Os(bpy)_2(CO)R]^+$ (R = Me, C_2H_5, or Ph). Values for k_1 were obtained for the series by assuming the same mechanism and by using the same kinetic analysis. As shown by the plot of ln k_1 vs the cone angle[7] of the R group in Figure 1D: (1) rate constants for the cis complexes have a remarkable dependence on the steric bulk of the group cis to CO, (2) although the stereochemically more crowded cis isomers are more sensitive to steric effects than are the trans isomers, they are intrinsically more reactive toward CO_2, and (3) if isomeric intermediates exist for the cis and trans series, they are stereochemically rigid under the conditions that lead to CO_2 reduction.

Finally, a comparison between our proposed mechanism of catalysis with that of Amatore and Saveant for the reduction of CO_2 in CH_3CN solution at a Pt electrode[8] is revealing in three ways. First, oxalate formation is the kinetically favored pathway for the uncatalyzed reduction with $k = 10^7$ M^{-1} s^{-1} for the coupling of CO_2^-, but this pathway is suppressed in the Os-catalyzed reaction, apparently as a consequence of CO_2 binding and the subsequent bimolecular reaction of sterically demanding intermediates. Second, for CO production, the dimerization of I_a replaces the reaction between CO_2^- and free CO_2 that occurs in the uncatalyzed system. Lastly, the formate making step is of similar form in both mechanisms, i.e., reaction of a proton with either CO_2^- or reduced, metal-complexed CO_2, followed by a rapid electron transfer from an external reductant, that is, CO_2^- in the uncatalyzed process or a reduced Os complex in the catalyzed process.

Acknowledgment. Financial support by the Gas Research Institute is greatly appreciated. Special thanks are due to Dr. C. Mark Bolinger for the development of the electrolysis techniques.

Registry No. *cis*-$[Os(bpy)_2(CO)H][PF_6]$, 84117-35-1; CO_2, 124-38-9; CO, 630-08-0; HCO_2^-, 71-47-6; *cis*-$[Os(bpy)_2(CO)H]^-$, 111437-23-1; *cis*-$[Os(bpy)_2(CO)CH_3]^-$, 111437-17-3; *cis*-$[Os(bpy)_2(CO)C_6H_5]$-$^-$, 111437-18-4; *cis*-$[Ru(bpy)_2(CO)CH_2C_6H_5]^-$, 111437-19-5; *cis*-$[(bpy)_2Os(CO)H]^+$, 84117-34-0; *cis*-$[(bpy)_2Os(CO)CH_3]^+$, 111437-20-8; *cis*-$[(bpy)_2Ru(CO)CH_2C_6H_5]^+$, 82482-59-5; *cis*-$[(bpy)_2Os(CO)C_6H_5]^+$, 111437-21-9; *trans*-$[(bpy)_2Os(CO)CH_3]^+$, 111554-34-8; *trans*-$[(bpy)_2Os(CO)CH_2CH_3]^+$, 111437-22-0; *trans*-$[(bpy)_2Os(Co)C_6H_5]^+$, 111554-35-9.

---

(6) (a) Feldberg, S. W. In *Electroanalytical Chemistry*; Bard, A. J., Ed.; Marcel Dekker: New York, 1969; Vol. 3. (b) Feldberg, S. W. In *Computer Applications in Analytical Chemistry*; Mark, H. B., Ed.; Marcel Dekker; New York, 1972; Vol. 2, Chapter 7. (c) Zizelman, P. M.; Amatore, C.; Kochi, J. *J. Am. Chem. Soc.* **1984**, *106*, 3771.

(7) Tolman, C. A. *Chem. Rev.* **1977**, *77*, 313.

(8) Amatore, C.; Saveant, J.-M. *J. Am. Chem. Soc.* **1981**, *103*, 5021.

Reaction of a Terminal Phosphinidene Complex with a Carbyne Complex. Synthesis and X-ray Crystal Structure of a Metallaphosphirene

Ngoc Hoa Tran Huy,[1a] Jean Fischer,[1b] and François Mathey*[1a]

Laboratoire de Chimie du Phosphore et
des Métaux de Transition, DCPH
Ecole Polytechnique, 91128 Palaiseau Cedex, France
and Laboratoire de Chimie des Métaux
de Transition et Catalyse, Institut Le Bel
Université Louis Pasteur, 67070 Strasbourg, France

Received July 29, 1987

Summary: The terminal phosphinidene complex $[PhP{=}W(CO)_5]$ as generated from the appropriate 7-phosphanorbornadiene complex reacts with the carbyne complex $PhC{\equiv}W(CO)_2Cp$ to give a three-membered tungstaphosphirene ring via a formal [1 + 2] P + W$\equiv$C cycloaddition.

In a previous note,[2] we described the condensation of a terminal phosphinidene[3] with a carbene complex. A η^1-P

---

[1] (a) Laboratoire de Chimie du Phosphore et des Métaux de Transition. (b) Laboratoire de Chimie des Métaux de Transition et de Catalyse.

[2] Tran Huy, N. H.; Mathey, F. *Organometallics* **1987**, *9*, 207.

0276-7333/88/2307-0240$01.50/0

Table I. Crystal Data

formula	$C_{25}H_{15}O_7PW_2$	cryst dimens (mm)	0.25 × 0.10 × 0.08
mol wt	826.07	radiation	Cu Kα graphite monochromated
cryst system	monoclinic	scan mode	$\theta/2\theta$ flying step–scan
a (Å)	9.276 (3)	scan angle, deg	$1.0 + 0.143 \tan \theta$
b (Å)	30.254 (8)	scan speed	0.024 deg s^{-1}
c (Å)	8.913 (3)	octants	$\pm hkl$
β (deg)	103.70 (2)	θ limits, deg	$4 < \theta < 55$
V (Å^3)	2430.2	no. of measurements	5259
space group	$P2_1/c$	no. of data with $I > 3\sigma(I)$	2725[a]
Z	4	abs min/max	0.70/1.65
d(calcd) (g cm^{-3})	2.258	$R(F)$	0.031
μ (cm^{-1})	184.81	$R_w(F)$	0.042
		GOF	1.33

[a] Many reflections were unobserved due to the low diffusion power of the crystal.

phosphaalkene complex was thus obtained via a transient metallaphosphirane (eq 1).

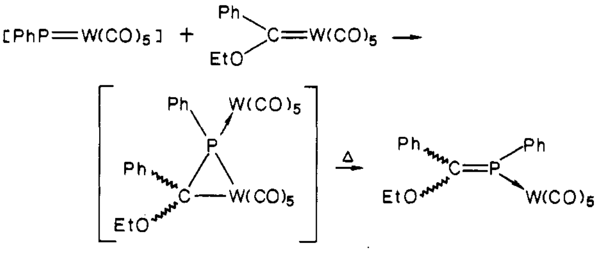

(1)

This preliminary success prompted us to extend our initial study to the carbyne case. Accordingly, equimolar amounts of the 7-phosphanorbornadiene complex 1 and the carbyne complex 2[4] were heated together in the presence of catalytic amounts of CuCl which is known to promote the decomposition of 1 at ca. 60 °C.[3] A stable metallaphosphirene P-W(CO)$_5$ complex, 3,[5] was thus produced (eq 2).

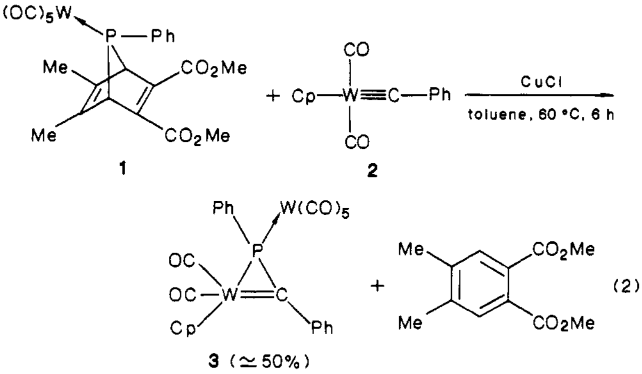

As far as we know, the only related structures that have ever been described in the literature[6,7] contain the tantalaphosphirene ring **4a** which, according to the X-ray data, seems to be best viewed as λ^5-phosphaalkyne η^2-complex **4b**.[7]

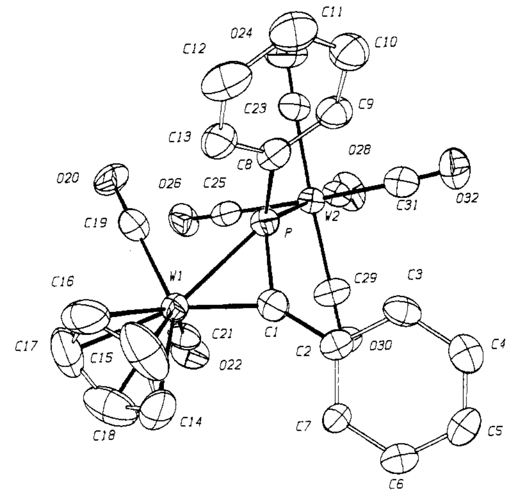

Figure 1. An ORTEP plot of one molecule of 3. Ellipsoids are scaled to enclose 50% of the electronic density. Hydrogen atoms are omitted. Principal bond lengths (Å): W1–C1, 1.954 (8); W1–P, 2.511 (3); P–C1, 1.775 (8); C1–C2, 1.47 (2); P–C8, 1.866 (8); W2–P, 2.522 (2). Principal bond angles (deg): P–W1–C1, 44.7 (2); W1–P–C1, 50.7 (2); W1–C1–P, 84.6 (3); W1–C1–C2, 146.6 (6); P–C1–C2, 128.7 (6); W1–P–W2, 127.52 (8); W1–P–C8, 110.6 (2); W2–P–C1, 120.2 (2); W2–P–C8, 119.5 (3); C1–P–C8, 107.7 (4).

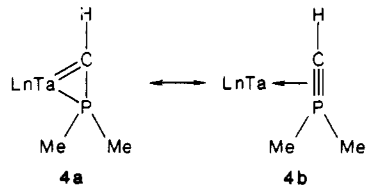

In our case, the X-ray crystal structure analysis of 3[8] is in favor of a genuine metallaphosphirene ring. Indeed, the P–C(Ph) bond length (1.775 Å) is very similar to the P–C(ring) bond length recorded in a phosphirene P-W(CO)$_5$ complex[9] and the W=C bond length is almost normal (1.95 Å vs 1.91 Å in a similar carbenic structure described by Stone[10]). In solution, the metallaphosphirene formulation

---

(3) For a recent review on the chemistry of terminal phosphinidene complexes, see: Mathey, F. *Angew. Chem., Int. Ed. Engl.* **1987**, *26*, 275.

(4) Fischer, E. O.; Lindner, T. L.; Huttner, G.; Friedrich, P.; Kreissl, F. R.; Besenhard, J. O. *Chem. Ber.* **1977**, *110*, 3397.

(5) Complex 3 was purified by chromatography on silica gel (eluent: pentane/CH_2Cl_2, 4/1): air-stable crystals; recrystallized from pentane/CH_2Cl_2; mp $\simeq$131 °C; ^{31}P NMR ($CDCl_3$) δ −188.7 ($^1J(^{31}P-^{183}W)$ = 259 Hz); ^1H NMR ($CDCl_3$) δ 5.83 (s, 5 H, Cp), 7.22 (m, 5 H, PhC), 7.50 (m, 3 H, PhP), 7.82 (d, ^3J(H–P) $\simeq$ 7.5 Hz, 2 H, PhP *ortho*); ^{13}C NMR ($CDCl_3$) δ 93.68 (s, Cp), 197.77 (d, ^2J(C-P) = 7.8 Hz, W(CO)$_5$ cis), 199.29 (d, ^2J(C–P) = 29.6 Hz, W(CO)$_5$ trans), 217.35–218.26 (2d, W(CO)$_2$), 266.34 (d, ^1J(C–P) = 54.3 Hz, C=W); IR (Decalin) ν(CO) 2070 (m), 1990 (s), 1940 (vs) cm^{-1}; mass spectrum (EI, 70 eV, ^{184}W) m/z (relative intensity) 826 (M$^+$, 11), 630 (M − 7CO, 78), 628 (100). Anal. Calcd for $C_{25}H_{15}O_7PW_2$: C, 36.35; H, 1.81; O, 13.56; P, 3.75; W, 44.52. Found: C, 36.53; H, 1.94; O, 13.27; P, 3.67; W, 44.07.

(6) Green, M. L. H.; Hare, P. M.; Bandy, J. A. *J. Organomet. Chem.* **1987**, *330*, 61 and references cited herein.

(7) Kee, T. P.; Gibson, V. C.; Clegg, W. *J. Organomet. Chem.* **1987**, *325*, C14.

(8) The diffraction data were collected at −100 °C on a Philips PW 1100/16 diffractometer. A parallepiped-shaped crystal was cut from a cluster and glued to a glass filament mounted on a rotation free goniometer head. Data collection parameters are given in Table I. The orientation matrix was obtained from 25 machine-centered reflections. Three standard reflections measured every hour showed no trend in intensity during data collection. The raw step–scan data were converted to intensities by using the Lehmann–Larsen[11] method and then corrected for Lorentz, polarization, and absorption factors, the latter computed by the empirical method of Walker and Stuart[12] since face indexation was not possible. The structure was solved by using Patterson techniques. After refinement of heavy atoms, difference Fourier maps revealed maxima of electron density close to the positions expected for hydrogen atoms. These atoms were introduced into structure factor calculations by their computed coordinates (C–H = 0.95 Å) and isotropic temperature factors such that $B(H) = 1 + B_{eqv}(C)$ Å^2. No hydrogen atom parameters was allowed to vary during full-matrix least-squares refinements minimizing $\sum w(|F_o| - |F_c|)^2$. The unit-weight observation in Table I is for $p = 0.08$ in $\sigma^2(F^2) = \sigma^2$ (counts) + $(pI)^2$. A final difference map showed no significant maxima. All computations were done on a MicroVax II computer using the SDP/VAX package.[13] The scattering factors were from ref 14 and 15, respectively.

(9) Marinetti, A.; Mathey, F.; Fischer, J.; Mitschler, A. *J. Am. Chem. Soc.* **1982**, *104*, 4484.

(10) Ashworth, T. V.; Chetcuti, M. J.; Howard, J. A. K.; Stone, F. G. A.; Wisbey, S. J. *J. Chem. Soc., Dalton Trans.* **1981**, 763.

(11) Lehmann, M. S.; Larsen, F. K. *Acta Crystallogr. Sect A: Struct. Crystallogr. Cryst. Chem.* **1974**, *A30*, 580.

is also supported by the extreme high-field shift of the ^{31}P resonance of **3** (δ −188.7 vs external 85% H_3PO_4) and by the low-field shift of the carbenic carbon ($\delta(^{13}C)$ + 266.3).

Registry No. **1**, 83603-06-9; **2**, 60635-78-1; **3**, 111495-74-0.

Supplementary Material Available: Anisotropic thermal parameters (Table S1), hydrogen atom parameters (Table S2), complete set of bond lengths (Table S3), and complete set of bond angles (Table S4) (8 pages); observed and calculated structure factor amplitudes for all observed reflections (×10) (Table S5) (11 pages). Ordering information is given on any current masthead page.

---

(12) Walker, N.; Stuart, D. *Acta Crystallogr., Sect. A.: Struct. Crystallogr. Cryst. Chem.* **1983**, *A39*, 158.

(13) Frenz, B. A. In *Computing in Crystallography*; Schenk, H., Olthof-Hazekamp, R., Van Koningsveld, H.; Bassi, G. C., Eds.; Delft University Press: Delft, The Netherlands, 1978; pp 64–71.

(14) Cromer, D. T.; Waber, J. T. *International Tables for X-Ray Cristallography*; Kynoch: Birmingham, England, 1974; Vol. IV, Table 2.2b.

(15) Cromer, D. T. *International Tables for X-ray Crystallography*; Kynoch: Birmingham, England, 1974; Vol. IV, Table 2.3.1.

Unexpected Formation of $[\mu\text{-}\eta^2\text{-(S)(S)}\underline{CSC_2H_4S}][\eta^1\text{-}\underline{CSC_2H_4S}]Fe_2(CO)_5$: Structure and Dynamic Behavior

Armelle Lagadec,[†] **Boguslaw Misterkiewicz,**[†]
André Darchen,[‡] **Daniel Grandjean,**[§]
Abdelhamid Mousser,[§] **and Henri Patin***[‖]

Laboratoire de Chimie des Organométalliques
Laboratoire d'Electrochimie, Laboratoire de Cristallochimie
et Ecole Nationale Supérieure de Chimie
University of Rennes, 35700-Rennes Beaulieu, France

Received January 21, 1987

Summary: Ethylene trithiocarbonate reacts with diiron nonacarbonyl to afford the coordination compound $[\mu\text{-}\eta^3\text{-S}\underline{CSC_2H_4S}]Fe_2(CO)_6$ in which the carbon of the thione is σ-bonded to one iron atom; upon warming, this complex is transformed into $[\mu\text{-}\eta^2\text{-(S)(S)}\underline{CSC_2H_4S}][\eta^1\text{-}\underline{CSC_2H_4S}]Fe_2(CO)_5$. The formation of this new coordination compound implies that the association of two fragments containing the heterocyclic moieties is followed by a redistribution of the sulfur atoms affording the planar carbenic ligand ($=\underline{CSC_2H_4S}$) and the original bridging system $[\text{(S)(S)}\underline{CSC_2H_4S}]$ in which a carbon atom is linked to four sulfur atoms.

Organic molecules containing the thiocarbonyl group are good ligands for zerovalent metal carbonyls and lead to families of mono- and polynuclear coordination compounds.[1] In this field we have shown that the behavior of the >C=S group toward diiron nonacarbonyl depends considerably on the nature of neighboring atoms. For instance, complexation of *O*-alkyl *S*-alkyl dithiocarbonate **1** affords compounds **3** in which the carbon atom of the thione is σ-bonded to one iron atom.[2] Upon warming or on electron-transfer catalysis, compound **3** rearranges to the carbenic binuclear complex **5**.[2,3] With trithiocarbonates **2** the fragmentation is not regiospecific and the two isomers **6** and **7** are obtained.[4] Finally, dithioesters **8** afford compounds **4** possessing a stable carbon–iron σ-bond.[5] All these coordination compounds are good models for study of the stereochemical aspects of ligand exchange under thermal activation or by electron-transfer catalysis.[6,7] Up to now, we have studied conformationally mobile sulfur ligands, but in this paper we describe the reactivity of the cyclic trithiocarbonate **9** which initially behaves like a dithioester ligand, affording **10**. Then **10**, under thermal activation, leads to the new compound **11**.

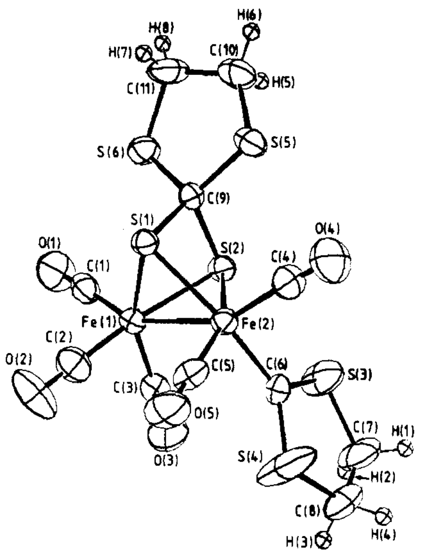

Figure 1. Molecular structure and labeling scheme for compound **11**. Relevant bond distances (Å) and angles (deg): Fe(1)–Fe(2), 2.489 (1); Fe(1)–S(1), 2.273 (2); Fe(1)–S(2), 2.275 (2); Fe(2)–S(1), 2.281 (2); Fe(2)–S(2), 2.282 (2); Fe(2)–C(6), 1.900 (6); S(1)–C(9), 1.850 (6); S(2)–C(9), 1.829 (6); S(3)–C(6), 1.680 (7); S(4)–C(6), 1.668 (7); S(5)–C(9), 1.803 (6); S(6)–C(9), 1.811 (6); Fe(1)–S(1)–Fe(2), 66.25 (5); Fe(1)–S(2)–Fe(2), 66.21 (5); Fe(2)–C(6)–S(3) 123.5 (4); Fe(2)–C(6)–S(4), 124.5 (4); S(3)–C(6)–S(4), 112.0 (4); S(1)–C(9)–S(2), 93.6 (3); S(1)–C(9)–S(5), 111.4 (3); S(1)–C(9)–S(6), 113.5 (3); S(2)–C(9)–S(5), 114.9 (3); S(2)–C(9)–S(6), 113.2 (3); S(5)–C(9)–S(6), 109.5 (3).

In contrast to the behavior of ligands of type **2**, the reaction of **9** with $Fe_2(CO)_9$ does not lead to the insertion of iron into a carbon–sulfur bond. Complex **10** was rapidly formed,[8] but the production of the more polar product **11**

[†] Laboratoire de Chimie des Organometalliques.

[‡] Laboratoire d'Electrochimie.

[§] Laboratoire de Cristallochimie.

[‖] Ecole Nationale Supérieure de Chimie.

(1) For a leading reference see: Seyferth, D.; Womack, G. B.; Cowie, M.; Hames, B. W. *Organometallics* **1984**, *3*, 1891.

(2) Lhadi, E. K.; Patin, H.; Darchen, A. *Organometallics* **1984**, *3*, 1128.

(3) Patin, H.; Mignani, G.; Benoit, A.; Le Marouille, J. Y.; Grandjean, D. *Inorg. Chem.* **1981**, *20*, 4351.

(4) Patin, H.; Mignani, G.; Mahe, C.; Le Marouille, J. Y.; Southern, T. G.; Benoit, A.; and Grandjean, D. *J. Organomet. Chem.* **1980**, *197*, 315.

(5) Patin, H.; Misterkiewicz, B.; Le Marouille, J. Y.; Mousser, A. *J. Organomet. Chem.* **1986**, *314*, 173.

(6) Darchen, A.; Lhadi, E. K.; Patin, H. *J. Organomet. Chem.* **1983**, *259*, 196.

(7) Darchen, A.; Mahe, C.; Patin, H. *Nouv. J. Chim.* **1982**, *6*, 539.

(8) To a solution of **9** (1.64 g, 12 mmol) in toluene (20 mL) was added 6 g of $Fe_2(CO)_9$ (16 mmol), and the mixture was allowed to react for 45 min at 55 °C under N_2 with stirring. The solvent was removed under vacuum and the residue chromatographed on silica plates (petroleum ether–diethyl ether (1/1)). The strips of R_f 0.6 and 0.3 were extracted and afforded, after crystallization, respectively 2.66 g of **10** (53%) and 1.05 g of **11** (19%). Compound **10** also is one of the components of the mixture obtained by irradiation[9] of $[Cr(CO)_5\{S\underline{CSC_2H_4S}\}]$ in the presence of $Fe(CO)_5$. **10**: mp 100–102 °C (pentane–ether) (lit.[9] mp 101–102 °C); mass spectrum, *m/z* calcd 415.786, found 415.786 ($M^{\cdot+}$), successive loss of six CO's, 248 ($C_3H_4S_3Fe_2$), 220 (CS_3Fe_2), 176 (Fe_2S_2), 144 (FeS), 136 ($C_3H_4S_3$); IR (Nujol) terminal carbonyl region 1950–2085 cm^{-1}; ^1H NMR ($CDCl_3$) δ 2.5 (m, 1 H), 3.45 (m, 3 H); ^{13}C NMR ($CDCl_3$ at 36 °C) δ 38.2 (CH_2), 49.5 (CH_2), 74.9 (CS), 208.7 (3 CO), 210.5 (3 CO). Anal. Calcd for $C_9H_4Fe_2O_6S_3$: C, 25.96; H, 0.96; S, 23.07. Found: C, 25.90; H, 0.89; S, 23.44.

0276-7333/88/2307-0242$01.50/0